Bruton's tyrosine kinase (BTK) regulates myeloid cell recruitment during acute inflammation

Gareth Purvis[1], Haidee Aranda[2], Keith Channon[1], and David Greaves[1]

[1]University of Oxford
[2]Sir William Dunn School of Pathology

May 3, 2021

Abstract

Bruton's tyrosine kinase (BTK) is a non-receptor kinase best known for its role in B lymphocyte development that is critical for proliferation, and survival of leukaemia cells in B cell malignancies. However, BTK is expressed in myeloid cells, particularly monocytes and macrophages where its inhibition has been reported to exhibit anti-inflammatory properties. Therefore, we explored the role of BTK on the migration of myeloid cells in vitro and in vivo. Using the zymosan induced peritonitis model of sterile inflammation we demonstrated that acute (1 h prior to zymosan) inhibition of BTK using a wide range of FDA (Ibrutinib and Acalabrutinib) and non-FDA approved inhibitors (ONO-4059, CNX-774, Olumatinib and LFM-A13) reduced neutrophil and monocyte recruitment. XID mice, which have a point mutation in the Btk gene had reduced neutrophil and monocyte recruitment to the peritoneum following zymosan challenge. To better understand the role of BTK in myeloid cell recruitment we investigated both chemotaxis and chemokine production in monocytes and macrophages. Pharmacological or genetic inhibition of BTK signalling substantially reduced human monocyte and murine macrophage chemotaxis to a range of chemoattractants (complement C5a and CCL2). We also demonstrated that inhibition of BTK in tissue resident macrophages significantly decreases chemokine secretion by reducing NF-kB activity and Akt signalling. Our work has identified a new role of BTK in regulating myeloid cell recruitment via two mechanisms, 1) reducing monocyte/macrophages' ability to undergo chemotaxis, and 2) reducing chemokine secretion, via reduced NF-kB activity in tissue resident macrophages.

Introduction

Inflammatory cell recruitment is a key step in the initiation of the acute immune response. Macrophage activation at the site of tissue injury results in the secretion of chemokines; these have a non-redundant role in leukocyte recruitment in pre-clinical models of inflammation. Activated macrophages are a major source of pro-inflammatory cytokines and chemokines in many chronic inflammatory diseases including rheumatoid arthritis, diet-induced diabetes or atherosclerosis (White et al., 2013). Chemokine-mediated recruitment, retention and activation of leukocytes, are attractive areas for the development of novel anti-inflammatory agents that could find application in a wide range of chronic inflammatory pathologies. We and others have demonstrated that genetic targeting of chemokine receptors shows promise in pre-clinical models of acute and chronic inflammation (McNeill et al., 2017). However, interventional studies in man using chemokine receptor antagonists have so far had limited therapeutic benefit (Schall and Proudfoot, 2011) (Noels et al., 2019). This could be due to high redundancy of chemokine receptor use in leukocytes to initiate monocyte/macrophage migration. Therefore, a therapeutic strategy that would affect both a myeloid cell's ability to undergo chemotaxis and reduced chemokine secretion could limit leukocyte recruitment by two independent but complementary mechanisms.

Bruton's tyrosine kinase (BTK) is a non-receptor bound intracellular signalling molecule best known for its signalling in B-cell development and malignancy. However, in recent years an alternative role for BTK is emerging in innate immune cells. BTK has been shown to be expressed at relatively high levels in myeloid

cells (Mangla et al., 2004). BTK is activated in monocytes and macrophages in numerous acute inflammatory conditions, including polymicrobial sepsis and cerebral ischaemia (O'Riordan et al., 2019a)(Ito et al., 2015) but also in chronic inflammatory conditions such as obesity-induced diabetes, rheumatoid arthritis and lupus (Purvis et al., 2020)(Honigberg et al., 2010)(Hartkamp et al., 2015). During the COVID-19 pandemic BTK has been shown to be activated in monocytes and intervention with the BTK inhibitor Acalabrutinib has been reported to reduce systemic inflammation in patients with severe COVID-19 (Roschewski et al., 2020). We and others have reported inhibition of BTK reduces NF-kB and the NLRP3 inflammasome activity in both murine and human macrophages, and reduces pro-inflammatory cytokine and chemokine production (O'Riordan et al., 2020)(Mao et al., 2020).

Pharmacological inhibition of BTK reduced macrophage accumulation in inflamed tissues in a pre-clinical model of type II diabetes (Purvis et al. 2020) and a model of cerebral ischaemia (Ito et al 2015). To confirm and extend these studies we tested the hypothesis that BTK can directly regulate myeloid cell recruitment to sites of inflammation. To do this we used a combination of *in vivo* and *in vitro* cell recruitment assays using a range of European medicines agency (EMA) or US Food and Drug administration (FDA) approved BTK inhibitors and tool compounds in combination with BTK-deficient X-linked immunodeficient (XID) mice. This allowed us to fully explore the magnitude and kinetics of myeloid cell recruitment in acute inflammation. We demonstrate that inhibition of BTK activity reduces neutrophil and monocyte recruitment via two independent but complementary mechanisms a) reducing monocyte chemotaxis, and b) reducing chemokine production from tissue resident macrophages.

Methods

Animals:

All animal studies were conducted with ethical approval from the Dunn School of Pathology Local Ethical Review Committee and in accordance with the UK Home Office regulations (Guidance on the Operation of Animals, Scientific Procedures Act, 1986). Male (8–12 weeks) C57BL/6J, CBA/CaCrl mice were obtained from Charles River Laboratories (Oxfordshire, UK). XID mice (CBA/CaHN-*Btk* ^{xid}/J) (Lindsley et al., 2007) are an inbred strain on the CBA background purchased from The Jackson Laboratory (#009361). They have a point mutation rendering the kinase domain of BTK inactive. Specifically, there is a C to T substitution at coding nucleotide 82, which alters the amino acid sequence; substituting an arginine for cysteine. The substitution is in a conserved PH domain and blocks the activation of the kinase (Rawlings et al., 1993) preventing BTK phosphorylation at Tyr^{223}, which is a key activating site. Importantly, ibrutinib binds irreversibly to Cys^{481}, also in the active site of the kinase domain and inhibits auto-phosphorylation of Tyr^{223}, thus blocking BTK activity. All mice were then housed in the same unit under conventional housing conditions at 25 ± 2°C and had access to food and water ad libitum.

Zymosan Induced peritonitis and flow cytometry:

C57BL/6J, CBA/CaCrl (WT) or CBA/CaHN-*Btk* ^{xid}/J (XID) mice were administered 100 µg zymosan A (Sigma-Aldrich) in PBS or vehicle intraperitoneally. After 2, 4, 16 or 48 h mice were sacrificed and peritoneal exudates collected by lavage with 7 ml of ice-cold sterile PBS with 5 mM EDTA. Total cell counts and cellular composition of peritoneal exudate were determined as previously described (Cash et al., 2009). Antibodies were used to identify neutrophils ($CD11b^+LyGC^+Ly6G^+$), monocytes ($CD11b^+LyGC^+Ly6G^-$) and B-cells ($CD11b^-BV220^+$) were purchased from Biolegend (San Diego, CA). Data was acquired using a BD LSRFortessa cytometer, and data analysed using FlowJo. Dosing regimen was determined from assessment of previously published doses of ibrutinib known to inhibit BTK *in vivo* (O'Riordan et al., 2019b), pre-dosing strategy was used as a proof of principle methodology for drug efficacy. Delivery route (oral gavage) has been previously demonstrated.

i) Ibrutinib pre-treatment dose response in 16 h ZIP

Male C57BL/6 mice (8 weeks old) were pre-treated with ibrutinib (0.1, 1 or10 $mg{\cdot}kg^{-1}$; p.o.) or vehicle (5% DMSO, 30% cyclodextrin) one hour prior to zymosan challenge (100 ug; i.p.). Peritoneal exudate cells were

harvested in ice-cold cell PEC harvest buffer (PBS, 5 mM EDTA) 16 h after zymosan challenge.

ii) Ibrutinib pre-treatment 48 h ZIP time course

Male C57BL/6 mice (10-12 weeks old) were pre-treated with ibrutinib (10 mg·kg^{-1}; p.o.) or vehicle (5% DMSO, 30% cyclodextrin) 1 hour prior to zymosan challenge (100 ug; i.p.). Peritoneal exudate cells were harvested in ice-cold PEC harvest buffer (PBS, 5 mM EDTA) 2, 4, 16 and 48 h after zymosan challenge.

iii) BTK inhibitors in 16 h ZIP model

Male C57BL/6 mice (10-12 weeks old) were pre-treated with ONO-4059, CNX-774, Olmutinib, LFM-A13, and Acalabrutinib (1 mg·kg^{-1}; p.o.) or vehicle (5% DMSO, 30% cyclodextrin) one hour prior to zymosan challenge (100 ug; i.p.). Compounds where all purchased from SellectChem, as selected because they had varying properties compared to ibrutinib i.e. more selective acalabrutinib, not marketed as a BTK inhibitor but target BTL Olmutinib, more potent ONO-4059 than ibrutinib and structurally different to ibrutinib CNX-774. All compounds also have publication history of being bioactive following oral gavage. Blood was collected by direct cardiac puncture and peritoneal exudate cells were harvested in ice-cold cell PEC harvest buffer (PBS, 5 mM EDTA) 16 h after zymosan challenge.

iv) Wild-type vs XID mice in 16 h ZIP model

Male CBA/CaCrl (WT) or XID mice (8-10 weeks old) were given zymosan challenge (100 ug; i.p.). Blood was collected by direct cardiac puncture, peritoneal exudate cells were harvested in ice-cold PEC harvest buffer (PBS, 5 mM EDTA) and spleen dissected 16 h after zymosan challenge.

Murine bone marrow-derived macrophages (BMDMs):

Bone marrow-derived macrophages were generated as previously described (Recio et al., 2018). Briefly, fresh bone marrow cells from tibiae and femurs of male C57BL/6 or XID mice aged 8–10 weeks were cultured in DMEM containing 4.5 g*L^{-1} glucose, 2 mM l-glutamine, 50 units*ml^{-1} penicillin and 50 µg·ml^{-1} streptomycin, 10% heat-inactivated FBS, 10% L929 cell-conditioned media (as a source of macrophage colony-stimulating factor) and for 7 days. Bone marrow cells were seeded into 8 ml of medium in 90 mm non-tissue culture treated Petri dishes (ThermoFisher Scientific, Sterilin, UK). On Day 5, an additional 5 ml of medium was added. Gentle scraping was used to lift cells. BMDMs were then counted and suspended in FBS free media at the desired cell concentration.

Murine resident peritoneal macrophage:

Peritoneal exudate cells were harvested in ice-cold PEC harvest buffer (PBS, 5 mM EDTA), cells were then pelleted and resuspended in DMEM (containing 4.5 g*L^{-1} glucose, 2 mM l-glutamine, 50 units*ml^{-1} penicillin and 50 µg·ml^{-1} streptomycin, 10% heat-inactivated FBS and allowed to attached to tissue culture treated plastic for 1 h. Unattached cells were washed off and cells stimulated as per experimental protocol.

Human monocyte isolation:

Human blood was obtained from healthy donors with informed consent and ethical approval in the form of leukocyte cones purchased from the NHS Blood and Transplant service. Leukocyte cones contain waste leukocytes isolated from individuals donating platelets via apheresis, and consist of a small volume (˜10 ml) of packed leukocytes with few red blood cells or platelets. For monocyte isolation, blood was diluted with 1:2 with PBS followed by separation using a Histopaque gradient and centrifugation as previously described (Purvis et al., 2020). Following human peripheral blood mononuclear cell (PBMC) isolation and washing, approximately 1 x 10^8 PBMCs were labelled and negatively selected using the pan human monocytes isolation kit and MACS separation (Miltenyi Biotec, Bisley, Surrey, UK). Monocytes were resuspended at 4 x 10^6 cells*ml^{-1} in chemotaxis buffer (RPMI 1640, 25 mM HEPES, 0.5% (w/v) BSA) and left on ice until required.

ACEA xCELLigence real-time cell migration:

Experiments were carried out with CIM-16 plates and an xCELLigence RTCA-DP instrument (ACEA, San Diego, USA) as previously described (Iqbal et al., 2013). Chemoattractants (complement C5a and CCL2, both purchased from Peprotech,UK) were made to desired concentrations (10 nM) in chemotaxis buffer (RPMI 1640/25 mM HEPES/0.5% (w/v) BSA) and loaded into the lower wells of the CIM-16 plate. Upper wells were filled with chemotaxis buffer and plates equilibrated for 30 min at RT. BMDM or human monocytes were resuspended in chemotaxis buffer and incubated with ibrutinib (1-30 μM) or vehicle (0.3 % DMSO) for 60 min at 37°C, 5% CO_2. Cell suspensions (BMDM; $2x10^6$/mL; hMonocytes; $4x10^6$/mL) were placed into the wells of the upper chamber, and the assay performed with recording of cellular impedance every 15 s for up to 8 h.

Macrophage NF-kB reporter cell line (RAW Blue)

A commercial macrophage reporter cell line (RAW Blue cells; InvivoGen, San Diego, CA; RRID:CVCL_X594) was used: Briefly, cells were derived from murine RAW 264.7 macrophages with chromosomal integration of a secreted embryonic alkaline phosphatase (SEAP) reporter construct, induced by NF-κB and activator protein 1 (AP-1) transcriptional activation. Cells were grown to 80 % confluence in DMEM containing 4.5 $g{\cdot}L^{-1}$ glucose, heat-inactivated 10 % FBS, 2 mM l-glutamine, and 200 $\mu g{\cdot}ml^{-1}$ Zeocin antibiotic (InvivoGen) at 37 degC in 5 % CO_2. To minimize experimental variability, only cells with fewer than five passages were used. Cells were plated at 0.95 x 10^5 per well. After experimental treatments, cell supernatants was added to 180 μl of QuantiBlue substrate (InvivoGen) and incubated at 37 °C for 60 min, plate was then read at an OD 655 nm (OD_{655}) on a microplate spectrophotometer (PherastarFSX, BMG Lab, UK).

MTT assay:

RAW Blue cell line viability was assessed by the mitochondrial metabolization of the tetrazolium salt 3-(4,5-methyltiazol- 2yl-)-2,5diphenyl-tetrazolium bromide] (MTT) (Applichen, Germany) colorimetric assay. Cells were maintained and plated as explained previously. The same treatment used for QuantiBlue assay was performed. Then MTT (0.5 $mg{\cdot}ml^{-1}$) was added, and cells were incubated at 37degC for 2 hours. Cell media was removed and formazan crystals were dissolved in DMSO. Optical density was measured at 570 nm (OD_{570}) on a microplate spectrophotometer (PherastarFSX, BMG Lab, UK).

ELISA:

Measurement of the protein levels of CXCL1 and CCL2 from peritoneal lavage fluids, or secreted into cell supernatants from 1.5 x 10^6 resident peritoneal macrophages was performed by ELISA (R&D Systems) according to the manufacturer's instructions.

Western Blotting:

Cells were lysed by adding RIPA buffer (Sigma-Aldrich) supplemented with protease and phosphatase inhibitors (Sigma, UK) followed by manual disruption. Protein concentration was determined by using a BCA protein assay kit (Thermo Fisher Scientific). Total cell protein (20 μg) was added to 4× Laemmli buffer (250 mM Tris–HCl, pH 6.8, 8 % SDS, 40 % glycerol, 0.004 % bromophenol blue, 20 % beta-mercaptoethanol) and heated at 72 °C for 10 min. Samples were then resolved on SDS-PAGE gels and transferred onto Hybond ECL nitrocellulose membranes (GE Healthcare, Buckinghamshire, UK). Membranes were blocked with 5% milk in Tris-buffered saline with Tween (TBS-T) (Tris-buffered saline, 0.1 % Tween-20) for 1h at RT and then incubated with the primary antibody (rabbit anti-phospho-BTK (Cell signalling 8714S), rabbit anti-total BTK (Cell signalling 8547S), rabbit anti-phospho-Akt (Cell signalling 4060S), rabbit anti-total Akt (Cell signalling 9272S) diluted 1:1,000 in 5% BSA/TBS-T overnight at 4°C. Next, membranes were incubated with an HRP-conjugated anti-rabbit secondary antibody for 1 h at RT. Protein bands were visualized by incubating the membranes for 5 min with Amersham ECL prime and subsequent exposure to X-ray film

over a range of exposure times. Western blotting of stripped membranes with an anti β-actin antibody (Cell Signalling) was used as a loading control. Densitometry was preformed using the Licor Studio Lite software.

Statistical analysis:

The data that support the findings of this study are available from the corresponding author upon reasonable request. Some data may not be made available because of privacy or ethical restrictions. All experiments were designed, where possible, to generate groups of equal size. Power calculations were used to estimate the group size based on an expected effect size of 30%. Where possible, blinding and randomisation protocols were used. All data in the text and figures are presented as mean ± standard error mean (SEM) of n observations, where$n$ represents the number of animals studied (*in vivo*) or independent values, not technical replicates (*in vitro*). Exclusion criteria was pre-determined before the beginning of experiment, if there was blood in the peritoneal at harvest an individual n would be excluded, or at analysis stage outliners were defined as greater than +/- 2 SD from the mean. For western blot data, all data are represented as fold change compared to mean control. All statistical analysis was calculated using GraphPad Prism 7 for Mac (GraphPad Software, San Diego, California, USA; RRID:SCR_002798). Statistical analysis was only undertaken for studies where each group size was at least $n = 4$. For western blot analysis, representative data are shown where group size is $n = 3$. When the mean of two experimental groups were compared, a two-tailed Students$t$ -test was performed. Normally distributed data without repeated measurements were assessed by a one-way ANOVA followed by Bonferroni correction if the F value reached significance. In all cases a$P < 0.05$ was deemed significant.

Results

Pre-treatment with ibrutinib prior to zymosan challenge reduces myeloid cell recruitment to the peritoneum.

Zymosan induced peritonitis (using 100 ug of zymosan) is a model of acute inflammation characterised by the recruitment of myeloid cells to the peritoneum following injection of zymosan, that is largely resolved after 48-96 h (Regan-Komito et al., 2017). To test if pharmacological inhibition of BTK with the FDA/EMA approved BTK inhibitor ibrutinib would reduce myeloid cell recruitment during acute inflammation C57BL/6 mice were pre-treated with ibrutinib (0.1 - 10 mg/kg; p.o.) 1 h prior to zymosan (100 ug; i.p.). Total peritoneal exudate cells were harvested 16h later and analysed using multicolour flow-cytometry. Total cellularity within the peritoneum increased significantly within 16 h of zymosan challenge (data not shown) and this mainly comprised of neutrophils ($CD11b^{+}Ly6C^{+}Ly6G^{+}$) (Figure 1A/C), monocytes ($CD11b^{+}Ly6C^{+}Ly6G^{-}$) (Figure 1A/D). As there is a resident population of B-cells in the peritoneum we also assessed B-cell number (Figure 1B). Ibrutinib treatment decreased total cellularity (Figure 1C), and significantly decreased neutrophil recruitment (Figure 1D) and monocytes recruitment (Figure 1E) into the peritoneum at 16 h, at all doses given compared to mice given vehicle prior to zymosan challenge. Importantly, ibrutinib treatment did not alter B-cells numbers within the peritoneum (Figure 1F). This result demonstrates for a direct role for BTK in myeloid cell recruitment *in vivo* .

Ibrutinib treatment 1 h prior to zymosan challenge reduces myeloid cell recruitment over a 48 h time course.

Having shown that ibrutinib treatment reduced both neutrophil and monocyte recruitment at 16h, we wanted to understand the full kinetics of myeloid cell recruitment over a 48 h time period. Mice were given ibrutinib (10 mg/kg; p.o.) 1 h prior to zymosan challenge and total peritoneal exudate cells harvested at 2, 4, 16 and 48 h. Following zymosan challenge there is rapid recruitment of cells into the peritoneum within the first 4 h (Figure 2A), of which the majority are $Ly6C^{+}Ly6G^{+}$ neutrophils (Figure 2B), this is followed by the peak infiltration of $Ly6C^{+}Ly6G^{-}$ monocytes at 16 h (Figure 2C). Ibrutinib treatment 1 h prior to zymosan challenge significantly reduced peak neutrophil recruitment at 2 and 4 h (Figure 2D/E). The initial peritoneal monocyte recruitment from the blood monocytes (2 and 4 h) was unaltered in ibrutinib treated mice (Figure 2H and I) but BTK inhibition significantly reduced the peak monocyte recruitment at 16 h and was maintained up to 48 h (Figure J and K). Overall, the magnitude of cellular recruitment is significantly

reduced in mice given a single ibrutinib treatment prior to zymosan challenge compared to mice given vehicle prior to zymosan challenge over the entire 48 h time frame studied (Figure 2 L-M).

Multiple BTK inhibitors reduce myeloid cell recruitment to the peritoneum and reduce recruitment to the blood from the spleen.

Having shown that ibrutinib, the first BTK inhibitor to gain FDA approval, inhibits neutrophil and monocyte recruitment to the peritoneum, we wanted to test a range of both more selective (Acalabrutinib) and less potent or more/less selective commercially available BTK inhibitors. All BTK inhibitors tested reduced cellularity in the peritoneum 16 h after zymosan challenge (Figure 3A). This was largely due to reductions in neutrophil accumulation (Figure 3B), while there was a similar trend in reducing monocyte accumulation (Figure 3C). We also measured myeloid cell numbers in the blood. Following zymosan challenge neutrophils and monocytes are mobilised to the blood from bone marrow or splenic reserves (Figure 3D). Overwhelmingly, mice treated with a BTK inhibitor prior to zymosan challenge had fewer neutrophils (Figure 3E) and monocytes (Figure 3F) in the blood at 16 h, the exception being Acalabrutinib pre-treatment which did not significantly alter neutrophil or monocyte mobilisation to the blood. These results collectively point to a central role in BTK in the regulation of neutrophil and monocyte recruitment *in vivo* .

XID mice have reduced myeloid cell recruitment to the peritoneum following zymosan challenge.

Having shown that multiple BTK inhibitors sequester/prevent monocytes from entering the blood and reduce peritoneal recruitment, we wanted to confirm the effects were BTK specific and not due to a common off-target effects of the BTK inhibitors used. Therefore, we used XID mice; which have a single point mutation in the *Btk* gene rendering the kinase domain inactive. XID mice and wild-type (WT) on the same background were injected with zymosan (100 µg; i.p.), which robustly initiated an acute inflammatory response characterised by an increase in total cellularity within the peritoneum (Figure 4A). Importantly, there was significantly less total cell recruitment to the peritoneum in XID mice injected with zymosan compared to WT mice injected with zymosan (Figure 4A). We next characterised the myeloid component of the recruited peritoneal exudate cells. When compared to WT mice challenged with zymosan, XID mice challenged with zymosan displayed significantly fewer $Ly6C^{+}Ly6G^{+}$ neutrophils (Figure 4B) and $Ly6C^{+}Ly6G^{-}$ monocytes (Figure 4C) in the peritoneum at 16 h. XID mice had significantly fewer B-cells in the peritoneum compared to WT mice, while zymosan challenge did not affect B-cell numbers (Figure 4D).

Neutrophils and monocytes are released into the circulation from the spleen following an inflammatory stimulus (Swirski et al., 2009), therefore, we wanted to investigate if BTK would regulate neutrophil and monocyte release from the spleen into the blood. We therefore quantified neutrophil and monocyte numbers in the blood and spleen. Following zymosan challenge there is an increase in the number of neutrophils in the blood in both WT and XID mice 16 h after zymosan challenge (Figure 4E), which is mirrored by an increase in the number of neutrophils in the spleen (Figure 4H). Following zymosan injection there is no alternation in circulating monocytes number in the blood (Figure 4F), however, there is a significant decrease in the number of monocytes in spleen in both WT and XID mice (Figure 4I). Within the spleen B-cell number was significantly increased following zymosan challenge in WT mice but was significantly lower in XID mice; no change in circulating B-cell levels in blood was observed following zymosan challenge in WT or XID mice (Figure 4G/J). These results tell us that BTK regulates monocyte/neutrophil recruitment to the circulation and to the site of inflammation.

We next wanted to confirm that the effects of ibrutinib treatment was BTK specific, to do this we pre-treated XID mice, with ibrutinib 1 h prior to zymosan challenge. Importantly there was no significant difference in cellular recruitment in XID mice treated with ibrutinib compared to XID treated with vehicle (Figure 4K); there was a very small but significant decrease in $Ly6C^{+}Ly6G^{+}$ neutrophil number in XID treated with ibrutinib (Figure 4L) and no difference in $Ly6C^{+}Ly6G^{-}$ monocyte recruitment (Figure 5M) and peritoneal B-cell number (Figure 4N). This finding strongly suggests that the BTK signalling is involved in neutrophils and monocyte recruitment during acute inflammation.

BTK regulates monocyte and macrophage chemotaxis.

Having shown that signalling through BTK is needed for myeloid cell recruitment *in vivo* we wanted to investigate if BTK regulated monocyte/macrophage ability to undergo chemotaxis. To address this question, we used a real-time chemotaxis assay (Iqbal et al., 2013). Murine bone marrow derived macrophages (BMDM) were pre-treated with ibrutinib (1-30 μM) for 60 min and allowed to migrate towards 10 nM complement C5a. Inhibition of BTK with ibrutinib reduced chemotaxis towards C5a in a concentration dependent manner (Figure 5A), as quantified by max-min analysis (Figure 5B) and area under the curve (AUC) (Figure 5C). To confirm this effect was BTK specific we generated BMDM from wild-type or XID mice and compared their ability to undergo chemotaxis towards C5a. BMDM from XID mice had significantly reduced ability to undergo chemotaxis towards C5a (Figure 5D) assessed by max-min analysis (Figure 5E) and AUC (Figure 5F). Having shown significant effects of BTK on murine macrophage chemotaxis, we next tested the actions of BTK inhibition on human monocyte chemotaxis. Monocytes were isolated by immunomagnetic selection from human leukocyte cones and pre-treated with ibrutinib (10 uM) or vehicle 1 h prior to assessment of their migratory capacity. Human monocytes treated with ibrutinib to inhibit BTK displayed significantly reduced ability to undergo chemotaxis towards CCL2 (Figure 5G), assessed by max-min analysis (Figure 5H) and AUC (Figure 5I) representative data for n=5 independent blood donation.

BTK ρεγυλατες μαςροπηαγε ςηεμοκινε προδυςτιον ια ΝΦ-κΒ.

We have previously shown that primary macrophages from XID mice or macrophages treated with ibrutinib *in vitro* secrete less pro-inflammatory cytokines in response to an inflammatory stimulus (Purvis et al., 2020). Therefore, we wanted to assess if following zymosan challenge *in vivo* , there was a reduction in chemokine levels in peritoneal lavage fluids. The initial wave of cellular recruitment to the peritoneum is dominated by neutrophils, therefore we assessed CXCL1 levels (a potent neutrophil chemoattractant) in peritoneal lavage fluids 1 h after zymosan challenge. Mice pre-treated with ibrutinib 1 h prior to zymosan challenge had significantly lower CXCL1 levels compared to mice treated with vehicle prior to zymosan challenge (Figure 6A). After the initial neutrophil recruitment there is an influx of monocytes, therefore we assessed CCL2 levels (a potent monocyte chemoattractant) in peritoneal lavage fluids after zymosan challenge. Mice pre-treated with ibrutinib 1 h prior to zymosan challenge had significantly lower CCL2 levels at 4 h (Figure 6B) and 16 h (Figure 6C) when compared to mice treated with vehicle prior to zymosan challenge. To prove that macrophages are the source of CXCL1 levels after zymosan challenge *in vivo* we isolated resident peritoneal macrophages and challenged them with zymosan for 1 h then measured secreted chemokine levels. Resident peritoneal macrophages treated with ibrutinib 1 h prior to zymosan challenge had reduced CXCL1 levels compared to vehicle treated (Figure 6D).

A key transcription factor that regulates pro-inflammatory gene expression in macrophages is NF-κB. Therefore, we investigated the ability of ibrutinib to inhibit NF-κB activity. Ibrutinib (0.1 - 30 μM) pre-treatment of RAW Blue cells inhibited NF-κB activity in a concentration dependant manner (Figure 6E). We next tested a range of BTK inhibitors (1μM); all the BTK inhibitors tested significantly inhibited NF-κB activity (Figure 6F). Only Olmutinib showed cellular toxicity at the concentration tested (Figure 6G). We next confirmed the ability of ibrutinib to inhibit phosphorylation of BTK in BMDM's. Pre-treatment of ibrutinib 1 h prior to LPS stimulation attenuated the increase in tyrosine phosphorylation on BTK (Figure 6H/I), which also resulted in decreased phosphorylation on Akt (Figure 6H/J). Taken together these data tell us that inhibition of BTK signalling reduces chemokine secretion from macrophages as a result of reduced NF-κB activity.

Discussion:

In this manuscript we report that inhibition of BTK signalling either pharmacologically or genetically reduces myeloid cell recruitment in acute inflammation. By using multicolour flow cytometry to accurately identify immune cell subsets and by performing a full kinetic analysis, rather than the single endpoint approaches, we were able to demonstrate the role of BTK throughout the acute inflammatory response. Our key findings were confirmed using two EMA/FDA approved BTK inhibitors, a range of structurally different BTK inhibitors

and BTK-deficient XID mice. Finally, we explored the mechanism(s) by which inhibition of BTK reduced myeloid cell recruitment during acute inflammation. We revealed two complementary mechanisms of action; a) inhibition of BTK reduced monocyte/macrophage chemotaxis to CCL2 and Complement C5a and b) inhibition of BTK reduced NF-ϰB dependent chemokine production from tissue resident macrophages.

Chemokines play a key role in monocyte recruitment and macrophage activation in pre-clinical models of human diseases characterised by chronic inflammation (McNeill et al., 2017). While genetic knockout mice of individual chemokine receptors give clear evidence for chemokines playing a non-redundant in inflammation, interventional studies in man using chemokine receptor antagonists has proven challenging with multiple drugs that target chemokine receptors failing to progress beyond early phase randomised clinical trials

However, as a cavate to this they suggest a lot of the negative data was due to inappropriate target selection and ineffective dosing. (Schall and Proudfoot, 2011). As an alternative to targeting single monocyte/macrophage chemoattractant GPCRs for therapeutic benefit, we and others have explored the potential of targeting multiple CC chemokines using the chemokine binding proteins (35 K-Fc) (McNeill et al., 2015) or lipoprotein molecules that inhibit monocyte chemotaxis towards CC chemokine (ApoA1) (Iqbal et al., 2016) or blocking macrophage responses to multiple chemoattractants (netrin) (van Gils et al., 2012). Here we target the non-receptor bound intracellular signalling molecule BTK. We clearly demonstrate that both pharmacological (Figure 1-3) and genetic inhibition of BTK signalling (Figure 4) limits myeloid cell recruitment during acute inflammation.

After an acute inflammatory stimulus there are usually two waves of immune cell infiltration (Marelli-Berg and Jangani, 2018). Neutrophils are rapidly recruited with peak infiltration 4-8 h after zymosan challenge, this is then followed by an infiltration of monocytes that peaks 16 h after zymosan challenge. Many anti-inflammatory drugs have been shown to reduce cellular infiltration in this model (Navarro-Xavier et al., 2010). In this report we show that BTK inhibitors have potent anti-inflammatory properties in a widely used model of sterile inflammation. In accordance with our data De Porto *et al.* report that ibrutinib treatment reduces PMN recruitment in acute pulmonary inflammation evoked by antibiotic-treated pneumococcal pneumonia and suggest that ibrutinib has the potential to inhibit ongoing lung inflammation in an acute infectious setting (de Porto et al., 2019). O'Riordan and colleagues reported reduced infiltration of neutrophils in a model of polymicrobial sepsis in XID mice (O'Riordan et al., 2020). Decreased myeloid cells recruitment has also been reported in other inflammatory models, RA, obesity and cerebral ischaemia, when BTK had been systemically inhibited with BTK inhibitors (Weber et al., 2017b). Taken together with our data these reports suggest that BTK inhibitors may represent novel therapeutic agent that could be used to reduce PMN recruitment in the setting of both acute and chronic inflammation.

One of the first steps in leukocyte recruitment is adhesion to and rolling along the vascular endothelium. While from XID mice have reduced neutrophil and monocyte recruitment to the peritoneum, neutrophils also appear to not be recruited as efficiently from the blood. Mueller*et al.* demonstrated using adhesion under flow experiments that BTK regulated E-selectin mediated slow rolling of neutrophils. In addition, they reported that downstream signalling of the BTK pathway divided into PLCγ2 and PI3Kγ-dependent pathways, both of which independently regulated β_2-integrin mediated adhesion (Mueller et al., 2010). We have extended these findings further demonstrating *in vivo* that genetic and pharmacological inhibition of BTK signalling significantly reduces neutrophil recruitment and now monocytes recruitment *in vivo* , giving further physiological relevance to these findings. It should be noted that BTK most likely only one of many interdependent mechanism by which monocytes and neutrophils facilitate directed movement along a chemotactic gradient.

Our experiments have shown for the first time that primary murine and human monocytes and macrophages have reduced ability to undergo real time chemotaxis to physiological relevant chemoattractants (CCL2 and C5a). Chemotaxis involves the directed movement of cells along a concentration gradient (Rumianek and Greaves, 2020). This movement involves cytoskeletal re-arrangement directed primarily by small Ras-like GTPases, cdc42 and Rac1 (Weber et al. 1998). In the formation of lamellipodia BTK has been shown to co-localise with Rac1 and Cdc42 (Nore et al. 2000). Additionally, BTK harbours pleckstrin homology

domains that allow it to interact with filamentous actin and BTK has been shown to co-localise with F-actin (Yao et al., 1999). A note of caution is that the afore mentioned work was carried out in B-cells. However, RNA Sequencing data generated from monocytes isolated from healthy donors and patients with XLA (inactive BTK) demonstrated differentially expressed novel lincRNAs that co-located with genes related to "Focal adhesion" and "Regulation of actin cytoskeleton" (Mirsafian et al., 2017). Collectively, these lines of evidence all point towards BTK having a key role in myeloid cell movement, having the ability to reduced cellular recruitment and chemotaxis by around 50 %. Our data proves that BTK signalling, in part, regulates neutrophil and monocyte recruitment *in vivo* and ability to undergo chemotaxis*in vitro* .

Macrophages are a major source of chemokine production following activation in both acute and chronic inflammation. We have shown that inhibition of macrophage BTK reduces cytokine and chemokine release both*in vitro* and *in vivo* in diabetes and poly microbial sepsis (Purvis et al. 2020; O'Riodan et al. 2020). A pro-inflammatory transcription factor that tightly regulates chemokine production is nuclear factor ϰ B (NF-kB); XID macrophages have poor induction of NF-kB following inflammatory stimulation (Mukhopadhyay et al., 2002). In this report we demonstrate that pharmacological inhibition of BTK reduces NF-ϰB and AP1 activity in WT macrophages, which is known to be a master transcription factor for the production of pro-inflammatory chemokine production. Pharmacological inhibition of NF-kB mediated cytokine and chemokine production has been shown to be beneficial in many acute and chronic pre-clinical disease models (Johnson et al., 2017)(Chen et al., 2017). Another selective BTK inhibitor, CGI1746, has been reported to reduce CCL2 levels from macrophages in myeloid cell–dependent arthritis by blocking trans-phosphorylation of BTK Tyr551 and subsequent auto-phosphorylation at Tyr223 (Di Paolo et al., 2011). Activated BTK trans-phosphorylates PLCγ2 on Tyr1217, one of the major regulatory residues involved in calcium mobilization needed for amongst other things cytokine release. Here we demonstrate that inhibition of BTK may have a beneficial effect in a wide range of inflammatory pathologies*in vivo* due to reducing chemokine production and therefore reducing myeloid recruitment which can exacerbate disease progression.

There has been a push in the last number of years to repurpose existing medicines for new therapeutic indication. There are a number benefits to this strategy as these medications have a) full safety profiles, b) significantly reduced cost than developing novel medication c) reduced cost to health care providers as many medications will be off patent and d) clinical data from existing patients who are taking these medications for other indication. This opens up an entire realm of possibility to repurpose existing mediations for new therapeutic indications. The recent COVID-19 pandemic saw a surge in pre-existing medications being trialled for the treatment of severe inflammatory syndromes, with the emergence of Dexamethasone (Sterne et al., 2020) and Tocilizummab (Group et al., 2021) from the RECOVERY Trial being recommended in the treatment of COVID-19. Indeed this opens up the possibility that new BTK inhibitors that are currently in pre-clinically studies many also be tested in disease modalities other than for B-cells malignancies (Langrish et al., 2021) . Our new data, along with numerous other reports, demonstrate that ibrutinib and acalabrutinib, which are both EMA/FDA approved medications, could be used in a wide range inflammatory conditions due to their potent anti-inflammatory effects' in myeloid cells; specifically, their ability to regulate myeloid cell recruitment, and reduce cytokine and chemokine production from macrophages, both of which are very tractable therapeutic targets. It should be noted that off target effects of ibrutinib have been reported to include atrial fibrillation, reoccurring infection and immunosuppression (Weber et al., 2017a). Of note, atrial fibrillation is not seen in patients treated with other BTK inhibitors and has attributed to inhibition of C-terminal Src kinase (Xiao et al., 2020). Impairments in leukocyte/platelet interaction have also been reported (Nicolson et al., 2020), however, this could be adventitious following acute myocardial infraction. While longer term use of tyrosine kinases is known to result in resistance. However, activation of myeloid cells is a key process in the pathology of many acute and chronic diseases so limiting this could have numerous advantages, but the most likely new use of a BTK inhibitors will in the treatment of acute inflammatory conditions for example sepsis, infection, abdominal aortic aneurysm (AAA) or myocardial infraction.

In conclusion we have demonstrated a novel role for BTK in regulating myeloid cell recruitment during acute inflammation. Specifically, we demonstrate a non-redundant role of BTK signalling in neutrophil and monocyte recruitment in a self-resolving model of sterile inflammation. Inhibition of BTK was able to

modulate myeloid cell recruitment by two independent but complementary mechanisms a) reducing monocyte chemotaxis to CCL2, and b) reducing chemokine production by tissue resident macrophages. Our data strengthen the case for using BTK inhibitors to reduce monocyte infiltration and macrophage activation in acute inflammatory diseases like sepsis or cardiovascular disease including myocardial infraction or stroke.

Author contribution and acknowledgements:

GSDP and DRG conceptualised the study. GSDP and HAT did the experimental work and analysed the data. GSDP drafted the manuscript. GSDP, HAT, KC and DRG reviewed and edited the manuscript. This work was funded by the British Heart Foundation Grant Number: RG/15/10/23915 to DRG and KC and a Pump Prime award from the Oxford British Heart Foundation Research Excellence: Grant Number: RE/13/1/30181 to GSDP and DRG. HAT was awarded a Maire Curie ERASUS Studentship and a PhD studentship from ULPGC University, Las Palmas Spain.

Cash, J.L., White, G.E., and Greaves, D.R. (2009). Chapter 17. Zymosan-induced peritonitis as a simple experimental system for the study of inflammation. Methods Enzymol. *461* : 379–96.

Chen, J., Kieswich, J.E., Chiazza, F., Moyes, A.J., Gobbetti, T., Purvis, G.S.D., et al. (2017). IkB kinase inhibitor attenuates sepsis-induced cardiac dysfunction in CKD. J. Am. Soc. Nephrol.*28* :.

Gils, J.M. van, Derby, M.C., Fernandes, L.R., Ramkhelawon, B., Ray, T.D., Rayner, K.J., et al. (2012). The neuroimmune guidance cue netrin-1 promotes atherosclerosis by inhibiting the emigration of macrophages from plaques. Nat. Immunol. *13* : 136–143.

Group, R.C., Horby, P.W., Pessoa-Amorim, G., Peto, L., Brightling, C.E., Sarkar, R., et al. (2021). Tocilizumab in patients admitted to hospital with COVID-19 (RECOVERY): preliminary results of a randomised, controlled, open-label, platform trial. MedRxiv 2021.02.11.21249258.

Hartkamp, L.M., Fine, J.S., Es, I.E. van, Tang, M.W., Smith, M., Woods, J., et al. (2015). Btk inhibition suppresses agonist-induced human macrophage activation and inflammatory gene expression in RA synovial tissue explants. Ann. Rheum. Dis. *74* : 1603–11.

Honigberg, L.A., Smith, A.M., Sirisawad, M., Verner, E., Loury, D., Chang, B., et al. (2010). The Bruton tyrosine kinase inhibitor PCI-32765 blocks B-cell activation and is efficacious in models of autoimmune disease and B-cell malignancy. Proc. Natl. Acad. Sci. U. S. A.*107* : 13075–80.

Iqbal, A.J., Barrett, T.J., Taylor, L., McNeill, E., Manmadhan, A., Recio, C., et al. (2016). Acute exposure to apolipoprotein A1 inhibits macrophage chemotaxis in vitro and monocyte recruitment in vivo. Elife*5* :.

Iqbal, A.J., Regan-Komito, D., Christou, I., White, G.E., McNeill, E., Kenyon, A., et al. (2013). A Real Time Chemotaxis Assay Unveils Unique Migratory Profiles amongst Different Primary Murine Macrophages. PLoS One *8* : e58744.

Ito, M., Shichita, T., Okada, M., Komine, R., Noguchi, Y., Yoshimura, A., et al. (2015). Bruton's tyrosine kinase is essential for NLRP3 inflammasome activation and contributes to ischaemic brain injury. Nat. Commun. *6* : 7360.

Johnson, F.L., Patel, N.S.A., Purvis, G.S.D., Chiazza, F., Chen, J., Sordi, R., et al. (2017). Inhibition of ϰB kinase at 24 hours after acute kidney injury improves recovery of renal function and attenuates fibrosis. J. Am. Heart Assoc. *6* :.

Langrish, C.L., Bradshaw, J.M., Francesco, M.R., Owens, T.D., Xing, Y., Shu, J., et al. (2021). Preclinical Efficacy and Anti-Inflammatory Mechanisms of Action of the Bruton Tyrosine Kinase Inhibitor Rilzabrutinib for Immune-Mediated Disease. J. Immunol.

Lindsley, R.C., Thomas, M., Srivastava, B., and Allman, D. (2007). Generation of peripheral B cells occurs via two spatially and temporally distinct pathways. Blood *109* : 2521–8.

Mangla, A., Khare, A., Vineeth, V., Panday, N.N., Mukhopadhyay, A., Ravindran, B., et al. (2004). Pleiotropic consequences of Bruton tyrosine kinase deficiency in myeloid lineages lead to poor inflammatory responses. Blood *104* : 1191–1197.

Mao, L., Kitani, A., Hiejima, E., Montgomery-Recht, K., Zhou, W., Fuss, I., et al. (2020). Bruton tyrosine kinase deficiency augments NLRP3 inflammasome activation and causes IL-1β–mediated colitis. J. Clin. Invest. *130* : 1793–1807.

Marelli-Berg, F.M., and Jangani, M. (2018). Metabolic regulation of leukocyte motility and migration. J. Leukoc. Biol. *104* : 285–293.

McNeill, E., Iqbal, A.J., Jones, D., Patel, J., Coutinho, P., Taylor, L., et al. (2017). Tracking Monocyte Recruitment and Macrophage Accumulation in Atherosclerotic Plaque Progression Using a Novel hCD68GFP/ApoE-/- Reporter Mouse-Brief Report. Arterioscler. Thromb. Vasc. Biol. *37* : 258–263.

McNeill, E., Iqbal, A.J., White, G.E., Patel, J., Greaves, D.R., and Channon, K.M. (2015). Hydrodynamic Gene Delivery of CC Chemokine Binding Fc Fusion Proteins to Target Acute Vascular Inflammation In Vivo. Sci. Rep. *5* : 17404.

Mirsafian, H., Ripen, A.M., Leong, W.-M., Chear, C.T., Mohamad, S. Bin, and Merican, A.F. (2017). Transcriptome profiling of monocytes from XLA patients revealed the innate immune function dysregulation due to the BTK gene expression deficiency. Sci. Rep. *7* : 6836.

Mueller, H., Stadtmann, A., Aken, H. Van, Hirsch, E., Wang, D., Ley, K., et al. (2010). Tyrosine kinase Btk regulates E-selectin–mediated integrin activation and neutrophil recruitment by controlling phospholipase C (PLC) γ2 and PI3Kγ pathways. Blood *115* : 3118–3127.

Mukhopadhyay, S., Mohanty, M., Mangla, A., George, A., Bal, V., Rath, S., et al. (2002). Macrophage effector functions controlled by Bruton's tyrosine kinase are more crucial than the cytokine balance of T cell responses for microfilarial clearance. J. Immunol. *168* : 2914–21.

Navarro-Xavier, R.A., Newson, J., Silveira, V.L.F., Farrow, S.N., Gilroy, D.W., and Bystrom, J. (2010). A new strategy for the identification of novel molecules with targeted proresolution of inflammation properties. J. Immunol. *184* : 1516–25.

Nicolson, P.L.R., Nock, S.H., Hinds, J., Garcia-Quintanilla, L., Smith, C.W., Campos, J., et al. (2020). Low-dose Btk inhibitors selectively block platelet activation by CLEC-2. Haematologica *106* : 208–219.

Noels, H., Weber, C., and Koenen, R.R. (2019). Chemokines as Therapeutic Targets in Cardiovascular Disease. Arterioscler. Thromb. Vasc. Biol.*39* : 583–592.

Nore, B.F., Vargas, L., Mohamed, A.J., Brandén, L.J., Brandén, B., Bäckesjö, C.-M., et al. Redistribution of Bruton's tyrosine kinase by activation of phosphatidylinositol 3-kinase and Rho-family GTPases.

O'Riordan, C.E., Purvis, G.S.D., Collotta, D., Chiazza, F., Wissuwa, B., Zoubi, S. Al, et al. (2019a). Bruton's Tyrosine Kinase Inhibition Attenuates the Cardiac Dysfunction Caused by Cecal Ligation and Puncture in Mice. Front. Immunol. *10* : 2129.

O'Riordan, C.E., Purvis, G.S.D., Collotta, D., Krieg, N., Wissuwa, B., Sheikh, M.H., et al. (2020). X-Linked Immunodeficient Mice With No Functional Bruton's Tyrosine Kinase Are Protected From Sepsis-Induced Multiple Organ Failure. Front. Immunol. *11* : 581758.

Paolo, J.A. Di, Huang, T., Balazs, M., Barbosa, J., Barck, K.H., Bravo, B.J., et al. (2011). Specific Btk inhibition suppresses B cell– and myeloid cell–mediated arthritis. Nat. Chem. Biol. *7* : 41–50.

Porto, A.P. de, Liu, Z., Beer, R. de, Florquin, S., Boer, O.J. de, Hendriks, R.W., et al. (2019). Btk inhibitor ibrutinib reduces inflammatory myeloid cell responses in the lung during murine pneumococcal pneumonia. Mol. Med. *25* : 3.

Purvis, G.S.D., Collino, M., Aranda-Tavio, H., Chiazza, F., O'Riordan, C.E., Zeboudj, L., et al. (2020). Inhibition of Bruton's TK regulates macrophage NF-ϰB and NLRP3 inflammasome activation in metabolic inflammation. Br. J. Pharmacol. *177* : bph.15182.

Rawlings, D.J., Saffran, D.C., Tsukada, S., Largaespada, D.A., Grimaldi, J.C., Cohen, L., et al. (1993). Mutation of unique region of Bruton's tyrosine kinase in immunodeficient XID mice. Science *261* : 358–61.

Recio, C., Lucy, D., Purvis, G.S.D., Iveson, P., Zeboudj, L., Iqbal, A.J., et al. (2018). Activation of the Immune-Metabolic Receptor GPR84 Enhances Inflammation and Phagocytosis in Macrophages. Front. Immunol.*9* :.

Regan-Komito, D., Valaris, S., Kapellos, T.S., Recio, C., Taylor, L., Greaves, D.R., et al. (2017). Absence of the Non-Signalling Chemerin Receptor CCRL2 Exacerbates Acute Inflammatory Responses In Vivo. Front. Immunol. *8* : 1621.

Roschewski, M., Lionakis, M.S., Sharman, J.P., Roswarski, J., Goy, A., Monticelli, M.A., et al. (2020). Inhibition of Bruton tyrosine kinase in patients with severe COVID-19. Sci. Immunol. *5* :.

Rumianek, A.N., and Greaves, D.R. (2020). How Have Leukocyte In Vitro Chemotaxis Assays Shaped Our Ideas about Macrophage Migration? Biology (Basel). *9* :.

Schall, T.J., and Proudfoot, A.E.I. (2011). Overcoming hurdles in developing successful drugs targeting chemokine receptors. Nat. Rev. Immunol. *11* : 355–363.

Sterne, J.A.C., Murthy, S., Diaz, J. V., Slutsky, A.S., Villar, J., Angus, D.C., et al. (2020). Association Between Administration of Systemic Corticosteroids and Mortality Among Critically Ill Patients With COVID-19. JAMA *324* : 1330.

Swirski, F.K., Nahrendorf, M., Etzrodt, M., Wildgruber, M., Cortez-Retamozo, V., Panizzi, P., et al. (2009). Identification of splenic reservoir monocytes and their deployment to inflammatory sites. Science *325* : 612–6.

Weber, A.N.R., Bittner, Z., Liu, X., Dang, T.-M., Radsak, M.P., and Brunner, C. (2017a). Bruton's Tyrosine Kinase: An Emerging Key Player in Innate Immunity. Front. Immunol. *8* : 1454.

Weber, A.N.R., Bittner, Z., Liu, X., Dang, T.-M., Radsak, M.P., and Brunner, C. (2017b). Bruton's Tyrosine Kinase: An Emerging Key Player in Innate Immunity. Front. Immunol. *8* : 1454.

Weber, K.S.C., Klickstein, L.B., Weber, P.C., and Weber, C. Chemokine-induced monocyte transmigration requires cdc42-mediated cytoskeletal changes.

White, G.E., Iqbal, A.J., and Greaves, D.R. (2013). CC chemokine receptors and chronic inflammation–therapeutic opportunities and pharmacological challenges. Pharmacol. Rev. *65* : 47–89.

Xiao, L., Salem, J.-E., Clauss, S., Hanley, A., Bapat, A., Hulsmans, M., et al. (2020). Ibrutinib-Mediated Atrial Fibrillation Attributable to Inhibition of C-Terminal Src Kinase. Circulation *142* : 2443–2455.

Yao, L., Janmey, P., Frigeri, L.G., Han, W., Fujita, J., Kawakami, Y., et al. (1999). Pleckstrin homology domains interact with filamentous actin. J. Biol. Chem. *274* : 19752–61.

Figure 1: Inhibition of BTK with ibrutinib 1 hour prior to zymosan challenge reduce myeloid cell recruitment to the peritoneum.

A) Representative flow cytometry plots of recruited neutrophils ($CD11b^+Ly6C^+Ly6G^+$) and recruited monocytes ($CD11b^+Ly6C^+Ly6G^-$) and **(B)** B-cells. **(C-F)** C57BL/6 mice were pre-treated with increasing dose of ibrutinib (0.1 - 10 mg/kg; p.o.) one hour prior to zymosan challenge (100 μg; i.p.) and peritoneal exudate cells harvested after 16 h. **(C)** Total peritoneal exudate cells were quantified as total cells proportional to counting beads from a defined volume of peritoneal lavage fluid **(D)** recruited neutrophils ($CD11b^+Ly6C^+Ly6G^+$),**(E)** recruited monocytes ($CD11b^+Ly6C^+Ly6G^-$) and **(F)** B-cells ($CD11b^-BV220^+$). Data shown are means ±

SEM of n=4 mice per group. $^{*}P < 0.05$, significantly different from Vehicle only; one-way ANOVA was performed with Bonferroni post hoc test.

Figure 2: Time course of peritoneal myeloid cell recruitment in mice treated with ibrutinib.

C57BL/6 mice were pre-treated with ibrutinib (10 mg/kg; p.o.) or vehicle one hour prior to zymosan challenge (100 μg; i.p.) and peritoneal exudate cells harvested after 2, 4, 16 and 48 h after zymosan challenge.**(A)** Total cell count in peritoneal exudate and quantified**(L)** , **(B)** number of recruited neutrophils ($CD11b^{+}Ly6C^{+}Ly6G^{+}$) and quantified **(M)** and **(C)** recruited monocytes ($CD11b^{+}Ly6C^{+}Ly6G^{-}$) and quantified **(N)** . Recruited neutrophils ($CD11b^{+}Ly6C^{+}Ly6G^{+}$) quantified at **(D)** 2h, **(E)** 4h, **(F)** 16 h and**(G)** 48 h. Recruited monocytes ($CD11b^{+}Ly6C^{+}Ly6G^{-}$) quantified at **(H)** 2h, **(I)** 4h, **(J)** 16 h and**(K)** 48 h. Data shown are means ± SEM n=6-12 mice per group.$^{*}P < 0.05$, $^{**}P < 0.01$, significantly different from Vehicle only; a student's t-test was performed when two groups are compared.

Figure 3: Inhibition of BTK reduces myeloid cell recruitment to the peritoneum and reduces recruitment to the blood from the spleen.

(A-C) C57BL/6 mice were pre-treated with a range of BTK inhibitors (10 mg/kg; p.o.) one hour prior to zymosan challenge (100 μg; i.p.) and peritoneal exudate cells harvest after 16 h. **(A)**Total peritoneal exudate cells were quantified, **(B)** recruited neutrophils ($CD11b^{+}Ly6C^{+}Ly6G^{+}$)and **(C)** recruited monocytes ($CD11b^{+}Ly6C^{+}Ly6G^{-}$).**(D-F)** Blood was harvested **(D)** total cellular count,**(E)** neutrophils ($CD11b^{+}Ly6C^{+}Ly6G^{+}$)and **(F)** monocytes ($CD11b^{+}Ly6C^{+}Ly6G^{-}$) counts assessed. Data shown are means ± SEM of n=5-6 mice per group.$^{*}P < 0.05$, $^{**}P < 0.01$, $P < 0.001$, $^{****}P < 0.0001$. significantly different from Vehicle only; one-way ANOVA was performed with Bonferroni post hoc test.

Figure 4: XID mice have reduced myeloid cells recruitment following zymosan challenge.

CBA/CaCrl (Wild-type) and XID mice challenged with zymosan (100 μg; i.p.) after 16 h peritoneal exudate cells **(A-D)** , blood**(E-G)** and spleens **(H-J)** harvested. **(A)** Total peritoneal exudate cells were quantified, **(B)** recruited neutrophils ($CD11b^{+}Ly6C^{+}Ly6G^{+}$) ,**(C)** recruited monocytes ($CD11b^{+}Ly6C^{+}Ly6G^{-}$) and **(D)** B-cells ($CD11b^{-}BV220^{+}$). Blood was harvested**(E)** total cellular count, (F) neutrophils ($CD11b^{+}Ly6C^{+}Ly6G^{+}$)and **(G)** monocytes ($CD11b^{+}Ly6C^{+}Ly6G^{-}$) counts assessed. **(H)** Total splenic cellular count, **(I)**neutrophils ($CD11b^{+}Ly6C^{+}Ly6G^{+}$)and **(J)** monocytes ($CD11b^{+}Ly6C^{+}Ly6G^{-}$) counts assessed. Data shown are means ± SEM of n=7-8 mice per group.$^{*}P < 0.05$, $^{**}P < 0.01$, $P < 0.001$, $^{****}P < 0.0001$; one-way ANOVA was performed with Bonferroni post hoc test, were there were multiple comparison or student's t-test where there appropriate.

Figure 5: Pharmacological or genetic inhibition of BTK reduces monocyte/macrophages chemotaxis.

(A) Bone marrow derived macrophages (BMDM) were incubated with ibrutinib (1-30 μM) for 60 min before being added to the upper chamber (1×10^5/well) of a CIM-16 plate and allowed to migrate 10 nM C5a. **(B)** BMDM from CBACaCrl or XID were added to the upper chamber (1×10^5/well) of a CIM-16 plate and allowed to migrate towards 10 nM C5a. **(C)** human monocytes were incubated with ibrutinib (10 μM) for 60 min before being added to the upper chamber (4×10^5/well) of a CIM-16 plate and allowed to migrate 10 nM CCL2. Combined traces of n=4-6 biological replicated are shown in panels (**A** , **D** , **G**). Migration was measured with max-min **(B, E, H)** analysis and area under the curve (**C** , **F** , **I**). Data expressed as mean + SEM, n = 4–6 biological replicates with 2 technical replicates per condition. Statistical analysis was conducted by one-way ANOVA with Dunnett's multiple comparison post-test. $^{*}P< 0.05$, $^{**}P < 0.01$, $P < 0.001$. relative to CCL2 or C5a alone. Or a student's t-test were appropriate.

Figure 6: BTK regulates **c** hemokines release from tissue resident macrophages by through NF-kB.

(A-C) C57BL/6 mice were pre-treated with ibrutinib (10 mg/kg; p.o.) or vehicle one hour prior to zymosan challenge (100 μg; i.p.) and peritoneal exudates were harvested after 1, 4 and 16 h after zymosan challenge. Levels of chemokines were measured in lavage fluids by ELISA**(A)** CXCL1 in 1 h, **(B)** CCL2 at 4 h and **(C)**CCL2 at 16 h. **(D)** Peritoneal macrophages were isolated from C57BL/6 mice and stimulated ex vivo

with zymosan and CXCL1 measured by ELISA. **(E-F)** NF-κB and AP1 activity assay in RAW Blue cells. Data shown mean ± SEM; n = 3-4 independent experiments with 4 technical replicated per condition. **(E)** Concentration response of ibrutinib (0.1-30 μM) pre-treatment 1 h prior to LPS stimulation.**(F)** a range of BTK inhibitors (1μM) given as a pre-treatment 1 h prior to LPS stimulation. **(G)** MTT assay of Raw Blue cells treated with BTK inhibitors for 6 h at 1 μM. **(H-J)** BMDM were pre-treated with ibrutinib (1 μM) 1 h prior to LPS stimulation and Tyr^{551} phosphorylation on BTK and Ser^{473} phosphorylation on Akt were assessed by western blot and quantified. Statistical analysis was conducted by one-way ANOVA with Dunnett's multiple comparison post-test.$^{*}P < 0.05$, $^{**}P < 0.01$, $P < 0.001$, $^{****}P < 0.0001$ compared to vehicle.

Figure 1: Varying doses of ibrutinib 1 hour prior to zymosan challenge reduce myeloid cell recruitment to the peritoneum.

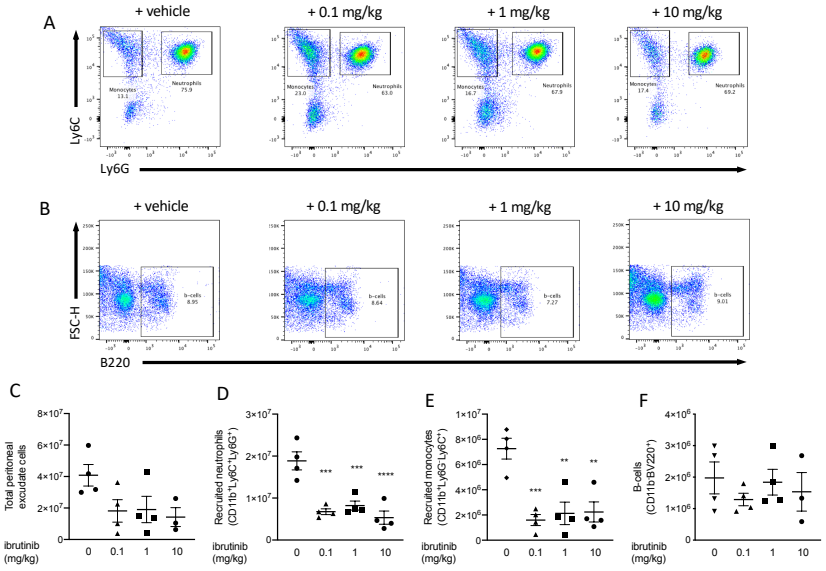

Figure 2: Time course of peritoneal myeloid cells recruitment in mice treated with ibrutinib.

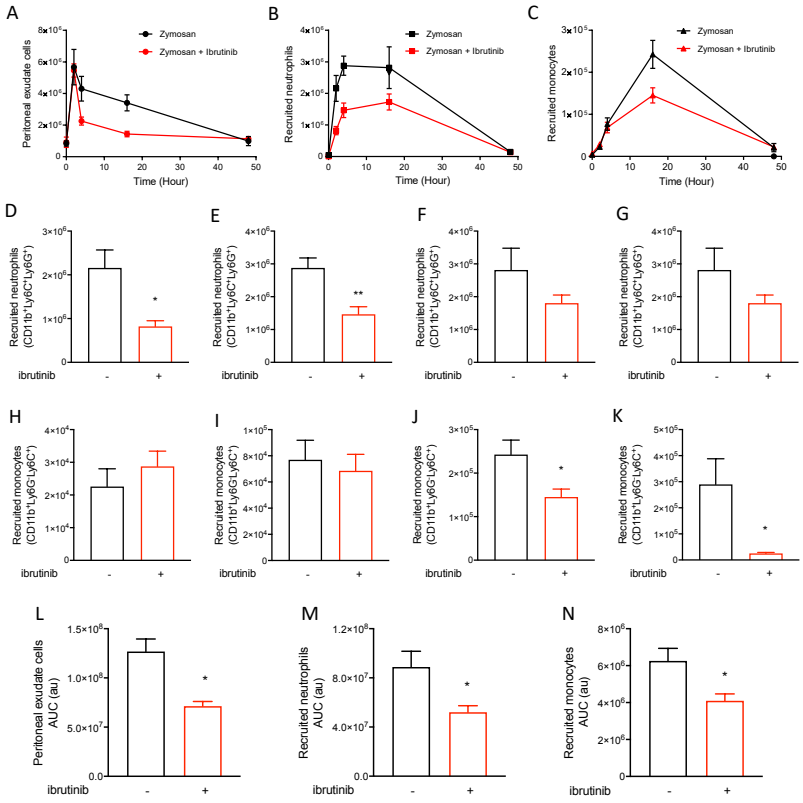

Figure 3: Inhibition of BTK reduces myeloid cell recruitment to the peritoneum, and reduces recruitment to the blood from the spleen.

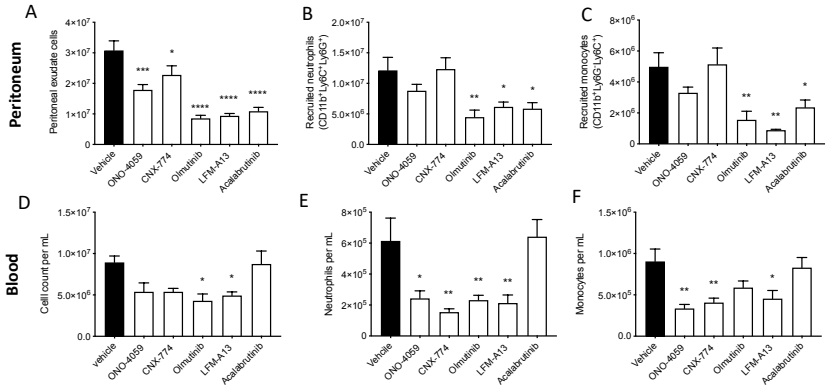

Figure 4: XID mice have reduced myeloid cell recruitment following zymosan challenge.

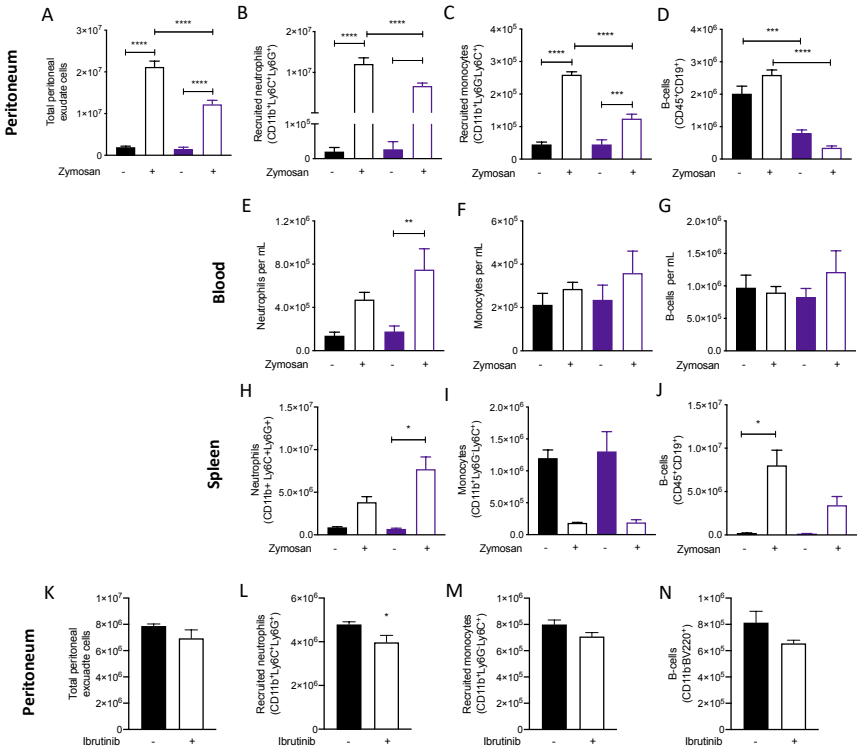

Figure 5: Pharmacological or genetic inhibition of BTK reduces monocyte/macrophages chemotaxis.

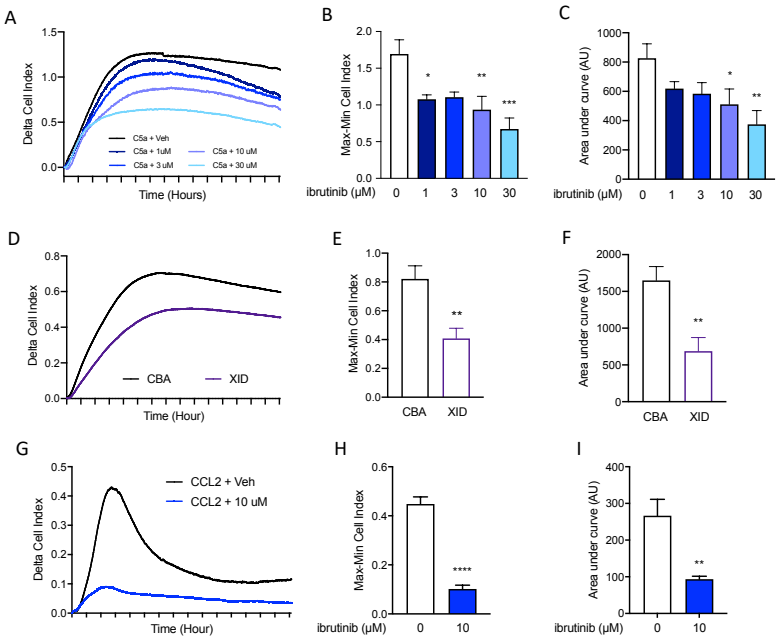

Figure 6: BTK regulates chemokines release from tissue resident macrophages by through NF-kB.